PROCEEDINGS OF SCIENCE

Improved currents for $\bar{B} \to D^{(*)}\ell\bar{\nu}$ form factors from Oktay-Kronfeld heavy quarks

arXiv:1411.4227v1 [hep-lat] 16 Nov 2014

Jon A. Bailey*, **Yong-Chull Jang, Weonjong Lee, Jaehoon Leem**
Lattice Gauge Theory Research Center, CTP, and FPRD
Department of Physics and Astronomy
Seoul National University, Seoul, 151-747, South Korea
E-mail: jonbailey@snu.ac.kr, wlee@snu.ac.kr

SWME Collaboration

The CKM matrix element $|V_{cb}|$ can be extracted by combining experimentally determined branching fractions for $\bar{B} \to D^{(*)}\ell\bar{\nu}$ decays with form factors from the lattice. While successful, the precision of this approach has been limited by heavy-quark discretization effects. An improved version of the Fermilab action, the Oktay-Kronfeld action, can be used to reduce heavy-quark discretization effects in calculations performed at the physical bottom and charm quark masses. Treating charm and bottom quarks as massive, we are carrying out improvement of the flavor-changing currents through third order in the momentum (HQET) expansion.

The 32nd International Symposium on Lattice Field Theory
23-28 June, 2014
Columbia University, New York, NY

*Speaker.

© Copyright owned by the author(s) under the terms of the Creative Commons Attribution-NonCommercial-ShareAlike Licence.

1. Introduction

The CKM matrix element $|V_{cb}|$ enters searches for new physics in the quark flavor sector of the Standard Model (SM). Parametric uncertainties from $|V_{cb}|$ dominate uncertainties in SM calculations of the branching ratios for the rare decays $K_L \to \pi^0 \nu\bar{\nu}$ and $B^0_{(s)} \to \mu^+\mu^-$, prime candidates for new physics, as well as SM calculations of the indirect CP violation parameter $|\varepsilon_K|$, which provides an input to the global unitarity triangle analysis.

The exclusive semileptonic decays $\bar{B} \to D^{(*)}\ell\bar{\nu}$ proceed at rates proportional to $|V_{cb}|^2$ [1, 2, 3, 4, 5].

$$\frac{d\Gamma}{d\omega}(\bar{B} \to D\ell\bar{\nu}) = \frac{G_F^2|V_{cb}|^2 M_B^5}{48\pi^3}(\omega^2-1)^{3/2} r^3 (1+r)^2 F_D^2(\omega)\,, \tag{1.1}$$

$$\frac{d\Gamma}{d\omega}(\bar{B} \to D^*\ell\bar{\nu}) = \frac{G_F^2|V_{cb}|^2 M_B^5}{4\pi^3}|\eta_{EW}|^2(1+\pi\alpha)(\omega^2-1)^{1/2} r^{*3}(1-r^*)^2 \chi(\omega) F_{D^*}^2(\omega)\,, \tag{1.2}$$

where $\omega = v_B \cdot v_{D^{(*)}}$ is the velocity transfer (proportional to the $D^{(*)}$ recoil energy, in the B rest frame), and $r^{(*)} = M_{D^{(*)}}/M_B$ is the ratio of the parent to the daughter meson mass. $\pi\alpha$ and η_{EW} are higher order electroweak corrections. $\pi\alpha$ is present only for the charged D^* and accounts for Coulomb attraction in the final state [3, 4, 5]. η_{EW} arises from NLO box diagrams in which a photon or Z is exchanged together with the W [2]. The kinematic factor $\chi(\omega)$ may be written

$$\chi(\omega) = \frac{\omega+1}{12}\left(5\omega + 1 - \frac{8\omega(\omega-1)r^*}{(1-r^*)^2}\right). \tag{1.3}$$

The form factors $F_{D^{(*)}}(\omega)$ are related to hadronic matrix elements of the flavor-changing currents. Compared to uncertainties in the form factors, uncertainties in the other quantities on the right-hand sides of Eqs. (1.1), (1.2) are small. At zero-recoil, $F_{D^*}(1) = h_{A_1}(1)$, and only the axial current matrix element contributes to the decay rate for $\bar{B} \to D^*\ell\bar{\nu}$; heavy quark symmetry implies $h_{A_1}(1) \approx 1$.

Given lattice QCD calculations of the form factors, experimental measurements of the decay rates yield determinations of $|V_{cb}|$. The value of exclusive $|V_{cb}|$ obtained in this way differs from the value obtained from the inclusive decays $\bar{B} \to X_c\ell\bar{\nu}$ and $\bar{B} \to X_s\gamma$ by 3.0σ. This difference is correlated with a 3.3σ tension between $|\varepsilon_K|$ in the SM and experiment [6]. This tension vanishes when inclusive $|V_{cb}|$ is used to calculate $|\varepsilon_K|$.

The form factors for the $\bar{B} \to D^{(*)}$ transition matrix elements are required for calculations, in and beyond the SM, of the ratios $R(D^{(*)}) \equiv \mathscr{B}(\bar{B} \to D^{(*)}\tau\bar{\nu})/\mathscr{B}(\bar{B} \to D^{(*)}\ell\bar{\nu})$, where $\ell = e, \mu$. The BaBar Collaboration reported a 3.4σ tension between its measurement of $(R(D), R(D^*))$ and the SM value [7]. This tension is only partially relieved by a lattice QCD calculation of $R(D)$ [8]. A lattice QCD calculation of the form factors for $\bar{B} \to D^*$ at non-zero recoil, required for lattice calculations of $R(D^*)$, does not (yet) exist.

The most precise determination of $|V_{cb}|$ to date was obtained with the form factor for $\bar{B} \to D^*\ell\bar{\nu}$ at zero recoil [9]. Charm-quark discretization effects dominate the uncertainty in the result. One way to reduce this systematic error is to generate data on finer lattices. An attractive alternative is to use a highly improved action. Two actions are of sufficient accuracy: the highly improved staggered quark (HISQ) action and the improved Fermilab action of Oktay and Kronfeld [10, 11].

The Oktay-Kronfeld (OK) action possesses the advantages of the Sheikholeslami-Wohlert (SW) action with the Fermilab interpretation, including control of discretization effects of fermions with arbitrary mass [12]. As $a \to 0$ or $m_Q \to \infty$, the discretization effects vanish, while discretization effects of bottom quarks are smaller than for charm quarks. These features enable direct validation of bottom sector calculations with calculations for the charm sector.

To reduce (heavy-quark) discretization effects in the axial and vector current matrix elements, one must improve not only the action, but also the currents. Following the work of Refs. [12, 13, 14, 15, 11], we introduce an improved field and are calculating quark-level matrix elements to fix the coefficients of the higher order operators, as functions of the bare quark masses. In Sec. 2 we briefly describe improvement for the current and write down a complete set of operators that can appear in the improved field, through third order in heavy quark effective theory (HQET). Section 3 contains a description of our matching calculations. In Sec. 4 we summarize completed and remaining work.

2. Improved field

The improvement program for fermions of arbitrary mass, in lattice units, begins with the observation that time-space axis interchange symmetry, a corollary of hypercubic rotation symmetry, is neither necessary nor convenient for constructing actions closer to the renormalized trajectory. Lifting time-space axis interchange symmetry in the SW action, including only higher-dimension operators that do not alter Wilson's time derivative, and appropriately specifying the coefficients in the action as functions of the fermion masses, one can systematically approach the renormalized trajectory even though the fermion masses are large compared to the lattice cutoff [12].

Improvement of other operators, including the flavor-changing currents, proceeds in much the same way. In Ref. [12], an improved field, coinciding with the canonical Dirac field at tree-level and through $\mathcal{O}(\boldsymbol{p})$, was introduced and shown to yield the desired continuum matrix elements (at tree-level and through $\mathcal{O}(\boldsymbol{p})$). Working at tree-level and to higher order in the momentum expansion, an improved field again suffices.

The OK action is improved through $\mathcal{O}(\boldsymbol{p}^3)$ in HQET power counting [11]. Accordingly, we begin with an ansatz for the improved field through $\mathcal{O}(\boldsymbol{p}^3)$,

$$\begin{aligned}\Psi_I(x) = e^{M_1/2}\Big[& 1 + d_1 \boldsymbol{\gamma}\cdot\boldsymbol{D} + \tfrac{1}{2} d_2 \triangle^{(3)} + \tfrac{1}{2} i d_B \boldsymbol{\Sigma}\cdot\boldsymbol{B} + \tfrac{1}{2} d_E \boldsymbol{\alpha}\cdot\boldsymbol{E} \\ & + \tfrac{1}{4} d_{rE} \{\boldsymbol{\gamma}\cdot\boldsymbol{D}, \boldsymbol{\alpha}\cdot\boldsymbol{E}\} + \tfrac{1}{4} d_{zE} \gamma_4 (\boldsymbol{D}\cdot\boldsymbol{E} - \boldsymbol{E}\cdot\boldsymbol{D}) + \tfrac{1}{6} d_3 \gamma_i D_i \triangle_i + \tfrac{1}{2} d_4 \{\boldsymbol{\gamma}\cdot\boldsymbol{D}, \triangle^{(3)}\} \\ & + \tfrac{1}{4} d_5 \{\boldsymbol{\gamma}\cdot\boldsymbol{D}, i\boldsymbol{\Sigma}\cdot\boldsymbol{B}\} + \tfrac{1}{4} d_{EE} \{\gamma_4 D_4, \boldsymbol{\alpha}\cdot\boldsymbol{E}\} + \tfrac{1}{4} d_{z3} \boldsymbol{\gamma}\cdot(\boldsymbol{D}\times\boldsymbol{B} + \boldsymbol{B}\times\boldsymbol{D})\Big] \psi(x)\,, \end{aligned} \tag{2.1}$$

where the rest mass M_1 is related to the bare quark mass, $\boldsymbol{D}$ is the symmetric lattice covariant derivative, $\triangle_i$ is a covariant lattice second derivative, $\triangle^{(3)}$ is the three-dimensional lattice Laplacian, $\boldsymbol{\Sigma}$ and $\boldsymbol{\alpha}$ are 4×4 matrices in spinor space, $\boldsymbol{B}$ and $\boldsymbol{E}$ are defined in terms of the clover field strength tensor, γ_μ are Euclidean gamma matrices, $\psi(x)$ is the unimproved field, and the coefficients d_i depend on the mass of the fermion ψ and other couplings in the action [12, 11]. The operators in this ansatz correspond to those in the OK action (bilinears) through mass dimension 6,

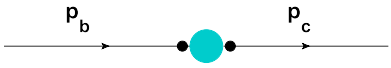

Figure 1: Diagram for quark-quark current matrix element for tree-level matching of the improved field. The matching yields the parameters d_i for $i = 1,2,3,4$.

including operators whose coefficients vanish at tree-level or are redundant. Hence, all operators allowed by the lattice symmetries are included.

The authors of Refs. [14, 15] showed explicitly that the currents constructed with the improved field through $\mathcal{O}(\boldsymbol{p})$, including only the d_1 term introduced in Ref. [12], coincides with that required to match through $\mathcal{O}(\Lambda_{\rm QCD}/m_Q)$ in HQET. To execute HQET matching, one enumerates operators in the lattice current that correspond to those of the effective continuum HQET. We have begun the task of extending this enumeration to third order in HQET.

3. Matching

Here we consider matching conditions to determine the coefficients in Eq. (2.1). The authors of Ref. [12] considered the quark-quark current matrix elements, Fig. 1, with the flavor-changing current inserted between external quarks. They noted that at tree-level the difference between lattice and continuum matrix elements is due to the difference between the lattice and continuum spinors and spinor normalization factors. Expanding the normalized continuum and lattice spinors through $\mathcal{O}(\boldsymbol{p})$ and comparing the lattice and continuum matrix elements yield d_1 (after equating the physical quark mass with the kinetic quark mass). Expanding the normalized continuum and lattice spinors through $\mathcal{O}(\boldsymbol{p}^3)$, we find

$$\sqrt{\frac{m_q}{E}}u(\xi,\boldsymbol{p}) = \left[1 - \frac{i\boldsymbol{\gamma}\cdot\boldsymbol{p}}{2m_q} - \frac{\boldsymbol{p}^2}{8m_q^2} + \frac{3i(\boldsymbol{\gamma}\cdot\boldsymbol{p})\boldsymbol{p}^2}{16m_q^3}\right]u(\xi,\boldsymbol{0}) + \mathcal{O}(\boldsymbol{p}^4)\,, \tag{3.1}$$

$$\mathcal{N}(\boldsymbol{p})u^{\rm lat}(\xi,\boldsymbol{p}) = e^{-M_1/2}\left[1 - \frac{i\zeta\boldsymbol{\gamma}\cdot\boldsymbol{p}}{2\sinh M_1} - \frac{\boldsymbol{p}^2}{8M_X^2} + \tfrac{1}{6}iw_3\sum_{k=1}^{3}\gamma_k p_k^3 + \frac{3i(\boldsymbol{\gamma}\cdot\boldsymbol{p})\boldsymbol{p}^2}{16M_Y^3}\right]u(\xi,\boldsymbol{0}) + \mathcal{O}(\boldsymbol{p}^4)\,, \tag{3.2}$$

where ξ labels the linearly independent solutions, $E = \sqrt{m_q^2 + \boldsymbol{p}^2}$, the index k is summed over the spatial directions,

$$\frac{1}{M_X^2} = \frac{\zeta^2}{\sinh^2 M_1} + \frac{2r_s\zeta}{e^{M_1}}\,, \qquad w_3 = \frac{3c_1 + \zeta/2}{\sinh M_1}\,, \tag{3.3}$$

$$\frac{1}{M_Y^3} = \frac{8}{3\sinh M_1}\left\{2c_2 + \frac{1}{4}e^{-M_1}\left[\zeta^2 r_s(2\coth M_1 + 1) + \frac{\zeta^3}{\sinh M_1}\left(\frac{e^{-M_1}}{2\sinh M_1} - 1\right)\right] + \frac{\zeta^3}{4\sinh^2 M_1}\right\}, \tag{3.4}$$

r_s is the coefficient of the spacelike Wilson term in the action, $\zeta = \kappa_s/\kappa_t$, $c_{1,2}$ are coefficients in the mass-dimension 6 terms of the OK action, which modify the lattice spinors and mass shell *via*

$$K_i = \zeta\sin p_i \quad\longrightarrow\quad K_i = \sin p_i\left[\zeta - 2c_2\sum_{j=1}^{3}(2\sin p_j/2)^2 - c_1(2\sin p_i/2)^2\right], \tag{3.5}$$

and the lattice spinor normalization factor for the OK action is

$$\mathcal{N}(\boldsymbol{p}) = \sqrt{\frac{\mu - \cosh E}{\mu \sinh E}} \quad \text{where} \quad \cosh E = \frac{1 + \mu^2 + \boldsymbol{K}^2}{2\mu}, \quad \text{and} \quad \boldsymbol{K}^2 = \sum_i K_i^2 \tag{3.6}$$

$$\mu = 1 + m_0 + \tfrac{1}{2} r_s \zeta \sum_{i=1}^{3} (2 \sin p_i/2)^2, \tag{3.7}$$

where m_0 is the bare heavy quark mass. As the lattice spacing tends to zero, the masses $M_{X,Y}$ tend to the rest mass M_1. With the OK action (matched at tree-level), the rotation breaking parameter $w_3 = c_B = r_s$. The mismatch between the lattice and continuum normalized spinors is compensated by the rotation parameters d_i in the current constructed from the improved field.

At tree-level the terms in Eq. (2.1) with chromoelectric and chromomagnetic fields do not contribute to the matrix elements of Fig. 1; only the terms with coefficients $d_{1,2,3,4}$ contribute. Setting the gauge links to one in the covariant derivatives, we note the additional factors entering contractions between differentiated fields and external quark states,

$$\psi \to \triangle^{(3)} \psi \;\text{ leads to }\; u^{\text{lat}} \to -\sum_i (2 \sin p_i/2)^2 u^{\text{lat}}, \tag{3.8}$$

$$\psi \to D_i \triangle_i \psi \;\text{ leads to }\; u^{\text{lat}} \to -i \sin p_i (2 \sin p_i/2)^2 u^{\text{lat}}, \tag{3.9}$$

$$\psi \to D_i \triangle^{(3)} \psi \;\text{ leads to }\; u^{\text{lat}} \to -i \sin p_i \sum_j (2 \sin p_j/2)^2 u^{\text{lat}}. \tag{3.10}$$

Then calculating the continuum and lattice matrix elements and demanding equality through $\mathcal{O}(\boldsymbol{p}^3)$,

$$\sqrt{\frac{m_c}{E_c}} \bar{u}_c(\xi_c, \boldsymbol{p}_c) \Gamma \sqrt{\frac{m_b}{E_b}} u_b(\xi_b, \boldsymbol{p}_b) = \mathcal{N}_c(\boldsymbol{p}_c) \bar{u}_c^{\text{lat}}(\xi_c, \boldsymbol{p}_c) \bar{R}(\boldsymbol{p}_c) \Gamma \mathcal{N}_b(\boldsymbol{p}_b) R(\boldsymbol{p}_b) u_b^{\text{lat}}(\xi_b, \boldsymbol{p}_b), \tag{3.11}$$

where $R(\boldsymbol{p})$ represents contributions from the improvement terms in Eq. (2.1) and depends on the parameters d_i. We find matching the $\mathcal{O}(\boldsymbol{p})$ terms yields d_1, matching the $\mathcal{O}(\boldsymbol{p}^2)$ terms yields d_2, matching the rotation breaking terms yields d_3, and matching the rotation invariant terms of $\mathcal{O}(\boldsymbol{p}^3)$ yields d_4. We have

$$d_1 = \frac{\zeta}{2 \sinh M_1} - \frac{1}{2 m_q}, \tag{3.12}$$

$$d_2 = d_1^2 - \frac{r_s \zeta}{2 e^{M_1}}, \tag{3.13}$$

$$d_3 = -d_1 + w_3, \tag{3.14}$$

$$d_4 = -\frac{d_1}{8 M_X^2} + \frac{d_2 \zeta}{4 \sinh M_1} + \frac{3}{16} \left(\frac{1}{M_Y^3} - \frac{1}{m_q^3} \right), \tag{3.15}$$

where m_q is to be taken equal to the kinetic mass M_2. The results for $d_{1,2}$ are contained already in Ref. [12].

To specify the remaining coefficients in Eq. (2.1), we are considering four-quark current matrix elements. For example,

$$\langle q^f(\xi_2, \boldsymbol{p}_2)\, c(\xi_c, \boldsymbol{p}_c) | J_\Gamma^{cb} | b(\xi_b, \boldsymbol{p}_b) q^g(\xi_1, \boldsymbol{p}_1) \rangle, \tag{3.16}$$

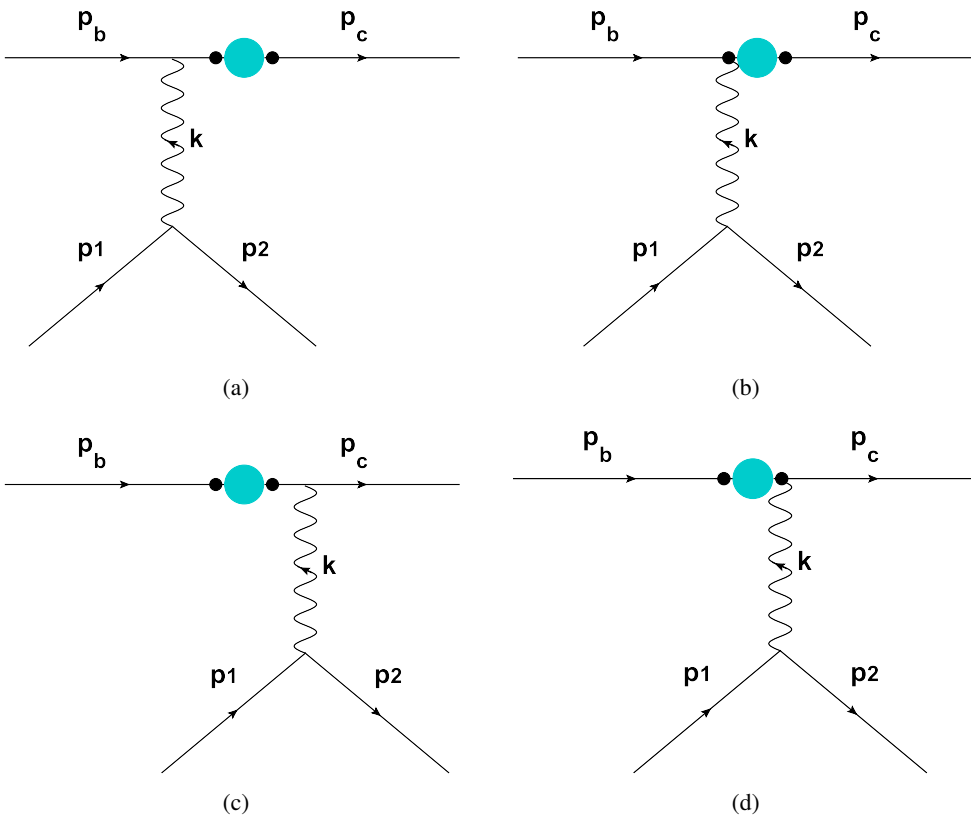

Figure 2: Diagrams for four-quark current matrix elements for tree-level matching of the improved field. The large circles are electroweak current insertions, and the small circles represent the field improvement terms.

where f, g are flavor indices and J^{cb}_{Γ} is the bottom (b) to charm (c) flavor-changing current. Tree-level diagrams contributing to this matrix element are shown in Fig. 2. The large filled circle is the current, and the small circles are the improvement terms. Gluon exchange can occur with the external bottom or charm quark or with the higher order operators in the improved bottom or charm field.

The OK action coefficients are specified (in part) through matching the quark-gluon vertex [11]. Turning to the current-gluon vertices and exchange with the external bottom and charm quarks, we expand in the external momenta. From the spatial component of the gluon vertex at lowest order, we recover the result for d_1, and we expect results for $d_{2,B}$ in agreement with Ref. [12]. From the time component and higher order terms in the momentum expansion, we anticipate information about the parameters d_E, d_{rE}, d_{zE}, d_5, d_{EE}, and d_{z3}.

The rotation parameters d_1, d_2, d_B, and d_E can also be obtained from the Foldy-Wouthuysen-Tani transformed field by including operators of $\mathcal{O}(\boldsymbol{p}^2)$ and matching the Hamiltonian [12]. We note that d_E cannot be altered by the higher order terms of $\mathcal{O}(\boldsymbol{p}^3)$ appearing in the OK action.

4. Summary

To reduce the discretization effects of heavy quarks, the OK action is improved through third

order in HQET power counting [11]. Systematic improvement of the hadronic $\bar{B} \to D^{(*)}$ matrix elements needed to extract $|V_{cb}|$ from the branching fractions of $\bar{B} \to D^{(*)}\ell\bar{\nu}$ decays requires improvement of the (axial and vector) $b \to c$ currents through the same order in HQET.

The authors of Ref. [12, 14, 15] showed that currents constructed from an improved quark field suffice for improvement of the hadronic matrix elements through $\mathcal{O}(\boldsymbol{p})$, or first order in HQET. The field improvement operators shown in Eq. (2.1) suffice for improvement of quark-quark current matrix elements, cf. Eq. (3.11). Matching to the continuum matrix elements yields the parameters $d_{1,2,3,4}$, Eqs. (3.12), (3.13), (3.14), and (3.15).

To specify the coefficients of the remaining operators, we are matching four-quark current matrix elements. To demonstrate improvement through third order in HQET, we are enumerating operators in the lattice currents and the (effective continuum) currents of HQET [14, 15].

Acknowledgments

J.A.B. is supported by the Basic Science Research Program of the National Research Foundation of Korea (NRF) funded by the Ministry of Education (No. 2014027937). The research of W. Lee is supported by the Creative Research Initiatives Program (No. 2014001852) of the NRF grant funded by the Korean government (MEST). W. Lee would like to acknowledge support from KISTI supercomputing center through the strategic support program for the supercomputing application research [No. KSC-2013-G2-005].

References

[1] A. V. Manohar and M. B. Wise, *Heavy quark physics*, *Cambridge* (2000).

[2] A. Sirlin *Nucl.Phys.* **B196** (1982) 83.

[3] E. S. Ginsberg *Phys.Rev.* **171** (1968) 1675.

[4] E. S. Ginsberg *Phys.Rev.* **162** (1967) 1570.

[5] D. Atwood and W. J. Marciano *Phys.Rev.* **D41** (1990) 1736.

[6] J. A. Bailey, Y.-C. Jang, and W. Lee *PoS* **LATTICE2014** (2014) 371, [1410.6995].

[7] J. Lees *et al. Phys.Rev.Lett.* **109** (2012) 101802, [1205.5442].

[8] J. A. Bailey and others [FNAL/MILC] *Phys.Rev.Lett.* **109** (2012) 071802, [1206.4992].

[9] J. A. Bailey and others [FNAL/MILC] *Phys.Rev.* **D89** (2014) 114504, [1403.0635].

[10] E. Follana and others [HPQCD/UKQCD] *Phys.Rev.* **D75** (2007) 054502, [hep-lat/0610092].

[11] M. B. Oktay and A. S. Kronfeld *Phys.Rev.* **D78** (2008) 014504, [0803.0523].

[12] A. X. El-Khadra, A. S. Kronfeld, and P. B. Mackenzie *Phys.Rev.* **D55** (1997) 3933–3957, [hep-lat/9604004].

[13] A. S. Kronfeld *Phys.Rev.* **D62** (2000) 014505, [hep-lat/0002008].

[14] J. Harada, S. Hashimoto, K.-I. Ishikawa, A. S. Kronfeld, T. Onogi, *et al. Phys.Rev.* **D65** (2002) 094513, [hep-lat/0112044].

[15] J. Harada, S. Hashimoto, A. S. Kronfeld, and T. Onogi *Phys.Rev.* **D65** (2002) 094514, [hep-lat/0112045].